Evidence for Redox Cooperativity between *c*-Type Hemes of MauG Which Is Likely Coupled to Oxygen Activation during Tryptophan Tryptophylquinone Biosynthesis†

Xianghui Li,‡ Manliang Feng,§ Yongting Wang,‡,|| Hiroyasu Tachikawa,§ and Victor L. Davidson*,‡

Department of Biochemistry, University of Mississippi Medical Center, Jackson, Mississippi 39216, and Department of Chemistry, Jackson State University, Jackson, Mississippi 39217

Received October 3, 2005; Revised Manuscript Received November 15, 2005

ABSTRACT: MauG is a novel 42 kDa diheme protein which is required for the biosynthesis of tryptophan tryptophylquinone, the prosthetic group of methylamine dehydrogenase. The visible absorption and resonance Raman spectroscopic properties of each of the two *c*-type hemes and the overall redox properties of MauG are described. The absorption maxima for the Soret peaks of the oxidized and reduced hemes are 403 and 418 nm for the low-spin heme and 389 and 427 nm for the high-spin heme, respectively. The resonance Raman spectrum of oxidized MauG exhibits a set of marker bands at 1503 and 1588 cm^{-1} which exhibit frequencies similar to those of the ν_3 and ν_2 bands of *c*-type heme proteins with bis-histidine coordination. Another set of marker bands at 1478 and 1570 cm^{-1} is characteristic of a high-spin heme. Two distinct oxidation−reduction midpoint potential (E_m) values of −159 and −244 mV are obtained from spectrochemical titration of MauG. However, the two ν_3 bands located at 1478 and 1503 cm^{-1} shift together to 1467 and 1492 cm^{-1}, respectively, upon reduction, as do the Soret peaks of the low- and high-spin hemes in the absorption spectrum. Thus, the two hemes with distinct spectral properties are reduced and oxidized to approximately the same extent during redox titrations. This indicates that the high- and low-spin hemes have similar intrinsic E_m values but exhibit negative redox cooperativity. After the first one-electron reduction of MauG, the electron equilibrates between hemes. This makes the second one-electron reduction of MauG more difficult. Thus, the two E_m values do not describe redox properties of distinct hemes, but the first and second one-electron reductions of a diheme system with two equivalent hemes. The structural and mechanistic implications of these findings are discussed.

MauG is a 42 kDa diheme protein (*1*) which is required for the biosynthesis of tryptophan tryptophylquinone (TTQ)[1] (*2*), the prosthetic group of methylamine dehydrogenase (MADH) (*3*). TTQ is synthesized through post-translational modification of two endogenous tryptophan residues. This modification involves two oxygenation reactions and one covalent cross-linking reaction. It has been shown that the incorporation of the second oxygen into βTrp^{57} and the covalent cross-linking of βTrp^{57} to βTrp^{108} are MauG-dependent processes (Figure 1). These reaction steps are severely compromised in vivo when *mauG* is mutated or deleted. Mutation of *mauG* in vivo leads to accumulation of a biosynthetic intermediate of TTQ in which βTrp^{57} is monohydroxylated and the covalent cross-link between βTrp^{57} and βTrp^{108} is absent (*4*). These steps may then be catalyzed in vitro upon addition of MauG to the isolated biosynthetic intermediate. Incubation of this biosynthetic intermediate in vitro with purified MauG results in the incorporation of the second oxygen into βTrp^{57} and formation of the cross-link with βTrp^{108} to form TTQ (*5*).

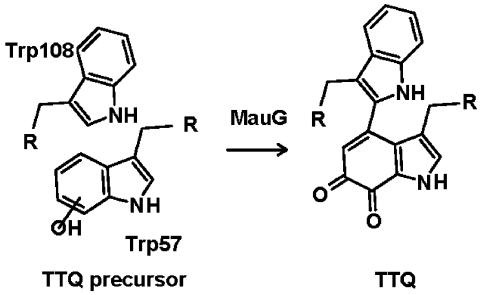

FIGURE 1: Role of MauG in tryptophan tryptophylquinone (TTQ) biosynthesis. This scheme is based on information from refs *4* and *5*.

The genes that encode the MADH subunits, together with nine other genes that relate to MADH expression and function, are clustered in the methylamine utilization (*mau*) locus (*6*, *7*). Four genes, *mauFEDG*, were shown to be essential for MADH maturation (*6*, *7*). The MauG protein is the only one of these gene products that has been expressed

† This work was supported by NIH Grants GM-41574 (V.L.D.) and S06G008047 (H.T.) and NIH-RCMI Grant 1G12RR12459-01 (H.T.).

* To whom correspondence should be addressed: Department of Biochemistry, University of Mississippi Medical Center, 2500 N. State St., Jackson, MS 39216-4505. Telephone: (601) 984-1516. Fax: (601) 984-1501. E-mail: vdavidson@biochem.umsmed.edu.

‡ University of Mississippi Medical Center.

§ Jackson State University.

|| Present address: Department of Chemistry, Massachusetts Institute of Technology, Cambridge, MA 02139.

[1] Abbreviations: MADH, methylamine dehydrogenase; TTQ, tryptophan tryptophylquinone; E_m, oxidation−reduction midpoint potential; NHE, normal hydrogen electrode; RR, resonance Raman; CV, cyclic voltammogram; SWNT, single-walled carbon nanotube.

10.1021/bi052000n CCC: $33.50
Published on Web 12/22/2005

and characterized (*1*). It contains two *c*-type hemes as predicted from its primary sequence, which contains two CXXCH motifs. In contrast to typical *c*-type cytochromes, the reduced form of MauG binds CO and is oxidized by O_2. The electron paramagnetic resonance spectrum of oxidized MauG exhibits signals corresponding to one high-spin heme and one low-spin heme. The *g* values exhibited by these hemes are atypical of *c*-type cytochromes and much more similar to those of hemes that bind and activate oxygen, such as ligand complexes of cytochrome P450CAM and the complex of heme oxygenase with heme.

The description of MauG-mediated TTQ biosynthesis in vitro demonstrated a novel function for this *c*-type heme protein, which is consistent with its physical properties that are atypical for a *c*-type heme protein. In this paper, we describe in detail the visible absorption and resonance Raman (RR) spectroscopic properties of each of the two *c*-type hemes, and the redox properties of MauG. The results indicate the high-spin heme and low-spin heme have very similar oxidation−reduction midpoint potential (E_m) values but exhibit negative cooperativity such that two distinct E_m values are obtained during the two-electron reduction of MauG. The structural and mechanistic implications of this unusual redox behavior are discussed.

MATERIALS AND METHODS

Materials. Homologous expression of MauG in *Paracoccus denitrificans* and methods for its isolation and purification have been described previously (*1*). All reagents were obtained from commercial sources and used without further purification.

Redox Titrations of MauG. Stoichiometric reduction and oxidation of MauG were performed anaerobically using sodium dithionite and potassium ferricyanide, respectively. Stock solutions of titrants were freshly prepared in 50 mM potassium phosphate (pH 7.4) which had been previously degassed and purged with nitrogen gas. The concentrations of titrants were standardized before and after MauG titrations by anaerobic titration against amicyanin, a protein standard with established redox properties (*8*) that is routinely used in our lab. The MauG sample was placed in a sealed cuvette and made anaerobic by repeated cycles of evacuation and argon replacement. Standardized solutions of titrants were quantitatively transferred with a gastight syringe, and the MauG sample was mixed with a stir bar at the bottom of the cuvette. Absorption spectra were recorded with a Multispec-1501 Shimadzu spectrophotometer.

Spectrochemical Titrations. The E_m values of MauG were determined by spectrochemical titration. The ambient potential was measured directly with a Corning combination redox electrode which was calibrated using quinhydrone (a 1:1 mixture of hydroquinone and benzoquinone) as a standard with an E_m value of 286 mV at pH 7.0 (*9*). The reaction mixture contained 5.0 μM MauG in 50 mM potassium phosphate buffer at pH 7.4 and 25 °C. Flavin mononucleotide and safranin T were present as mediators. The mixture was titrated by addition of incremental amounts of dithionite, which was used as a reductant. The reaction was fully reversible. In the oxidative direction, titration by addition of potassium ferricyanide was performed. The absorption spectrum of MauG and the ambient potential were recorded after each incremental addition of reductant or oxidant. The concentrations of the oxidized and reduced MauG were determined by comparison with the spectra of the completely oxidized and reduced forms of MauG after the absorbance of mediators was subtracted from the recorded spectrum. E_m values were obtained by fitting the experimental data to the following equations which describe the redox behavior of a system with either a single redox active component (eq 1) or two distinct redox active components (eq 2)

$$\text{fraction reduced} = 1/[1 + 10^{(E-E_m)/0.059V)}] \quad (1)$$

$$\text{fraction reduced} = a/[1 + 10^{(E-E_{m1}/0.059V)}] + (1 - a)/[1 + 10^{(E-E_{m2})/0.059V)}] \quad (2)$$

where a is the fraction of the total absorbance change that is attributable to one heme and $1 - a$ is the fraction of the total absorbance change that is attributable to the other heme. E_m values are reported versus the normal hydrogen electrode (NHE).

Direct Electrochemical Analysis. A CH Instruments model CHI 660A electrochemical workstation was used for recording cyclic voltammograms (CVs) of MauG with a three-electrode cell consisting of a saturated Ag/AgCl reference electrode (Ag/AgCl), a Pt wire auxiliary electrode, and a single-walled carbon nanotube (SWNT) coated glassy carbon disk working electrode (CH Instruments, 3 mm diameter). The working electrode was modified with SWNT which are pretreated with a 3:1 (v/v) solution of concentrated sulfuric acid (98%) and concentrated nitric acid (70%) as reported in the literature (*10*). E_m values are reported versus the NHE.

Resonance Raman Spectroscopy. Resonance Raman (RR) spectra were obtained using a Raman spectrometer consisting of a Spex model 1877 triple spectrograph and a CCD detector as reported previously (*11*). The protein solution was placed in a homemade flow system and maintained at a constant flow during the experiment to prevent laser-induced damage. A 406.7 nm line from a argon−krypton ion laser (Spectra-Physics BeamLok model 2080-KV) was used as the excitation source, and the Raman signal was collected in a 120° geometry. The laser power was adjusted to ~6 mW at the sample. Each spectrum was recorded with a 30 s accumulation time, and 15 repetitively measured spectra were averaged to improve the quality of the final spectrum. The frequencies of the Raman bands were calibrated using a standard argon lamp.

RESULTS

Visible Absorption Spectroscopy of Different Redox States of MauG. It was previously demonstrated that MauG possesses two covalently bound hemes per protein molecule and that reduction of the protein, as monitored by the visible absorption spectrum of the heme cofactors, requires two electron equivalents. In this study, stoichiometric titration of MauG was performed in an attempt to resolve the spectral features of each of the two hemes. MauG was titrated in both the reductive and oxidative directions, and difference spectra were generated after each incremental addition of titrant (Figure 2). As can be seen in Figure 2B, the changes in the overall two-electron titration appear to be monophasic. However, the difference spectra reveal a distinct shoulder

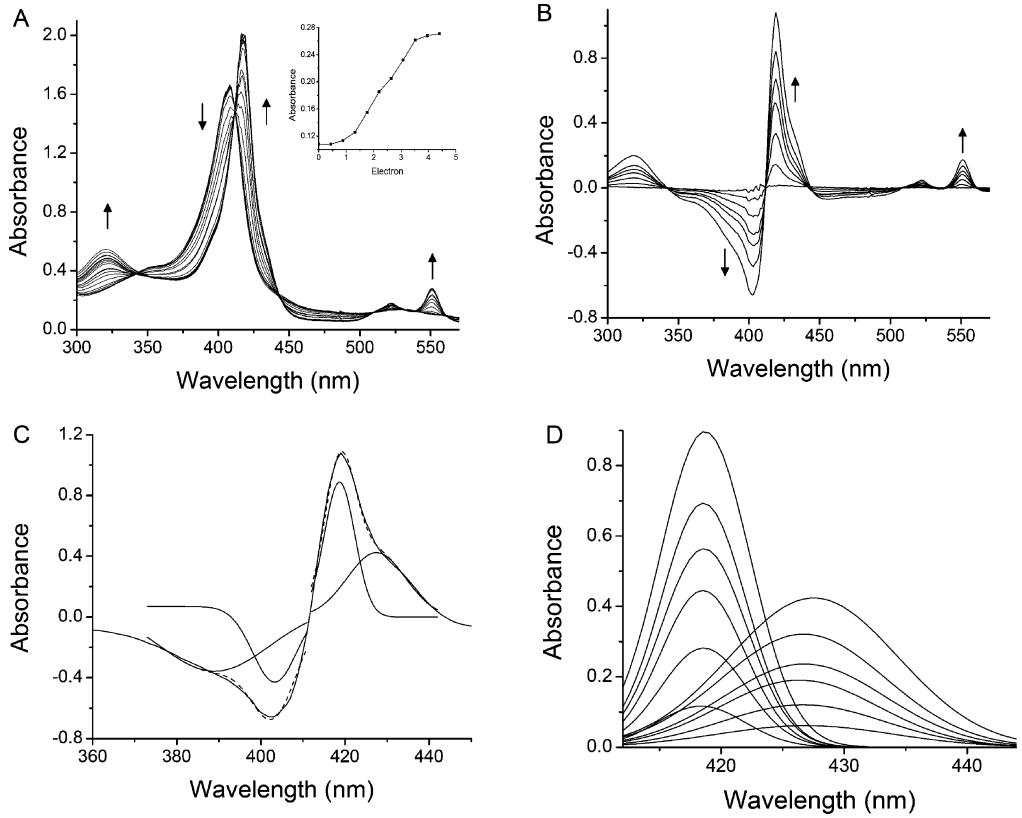

FIGURE 2: Anaerobic reductive titration of MauG with sodium dithionite. (A) Complete reduction by dithionite. The sample contained 7.9 μM MauG in 50 mM potassium phosphate (pH 7.4). Spectra were recorded after incremental additions of sodium dithionite. The arrows indicate the direction of the spectral changes during the titration. The change in absorbance at 550 nm upon addition of electron equivalents in the form of added dithionite is shown in the inset. (B) Reduced minus oxidized difference spectra. In this representation of the data depicted in panel A, the spectrum of the fully oxidized MauG was subtracted from each spectrum that was obtained after each addition of dithionite. (C) The individual components of the Soret peaks in the fully reduced minus oxidized spectrum were deconvoluted by Gaussian fitting with Origin 7.0. Each of the two fitted components is drawn under the original spectrum, and the overall fit of the sum of the two is drawn as a dashed line which overlays the original spectrum. (D) Deconvoluted spectra of the Soret peaks in reduced minus oxidized difference spectra shown in panel B.

in the Soret peak which suggests that the two heme components have distinct spectral properties. To observe this more clearly, the individual components of the Soret peaks in the fully reduced minus fully oxidized difference spectrum were deconvoluted by Gaussian fitting (Figure 2C). This revealed that in the reduced form of MauG the two hemes have Soret peaks at 418 and 427 nm and in the oxidized form of MauG the two hemes have Soret peaks at 403 and 389 nm. On the basis of typical known values for the absorption maxima of high- and low-spin hemes, one may conclude that the low-spin heme exhibits maxima at 403 and 418 nm and that the high-spin heme exhibits maxima at 389 and 427 nm for the ferric and ferrous forms, respectively. In theory, the two hemes of MauG could be reduced sequentially or at the same time. To examine this, the changes in Soret peaks which were obtained from the deconvoluted difference spectra during the course of the redox titration shown in Figure 2B were monitored. Figure 2D clearly shows that both of the deconvoluted Soret peaks of each heme attributable to the ferrous forms of the low-spin and high-spin hemes are each increasing in magnitude at approximately the same time. This indicates that the two hemes of MauG have similar E_m values.

Resonance Raman Spectroscopy of Different Redox States of MauG. The RR spectra of oxidized MauG, cytochrome *c*, and myoglobin are shown and compared in Figure 3. The RR spectrum of MauG much more closely resembles that

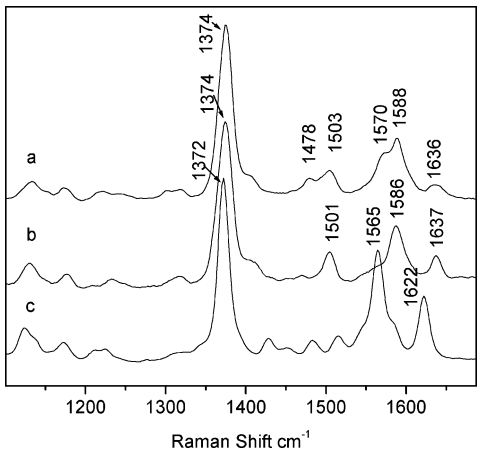

FIGURE 3: Resonance Raman spectra of MauG (a), cytochrome *c* (b), and myoglobin (c). Protein concentrations were 0.25 mM.

of cytochrome *c* since most of the major marker bands have similar frequencies and intensities. This result further confirms that MauG is a *c*-type heme protein despite physical properties that are atypical of cytochromes *c* and more typical of oxygen-binding hemes (*1*). With 406.7 nm excitation, the spectrum of MauG obtained at pH 7.5 shows two ν_3 bands at 1503 and 1478 cm^{-1}, two ν_2 bands at 1570 and 1588 cm^{-1}, and a ν_4 band at 1374 cm^{-1}. These marker bands, which are sensitive to the spin and coordination states of the heme iron, along with the slightly broad ν_{10} band at ~1636 cm^{-1} reveal

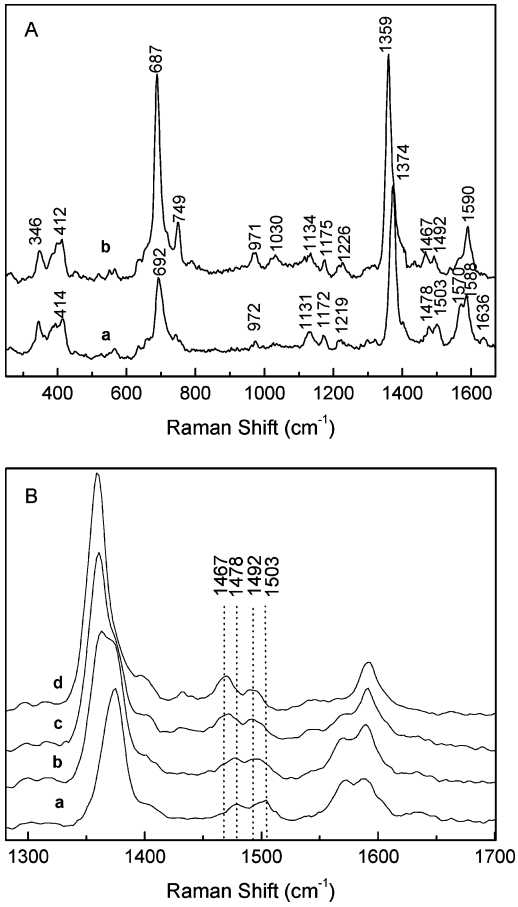

FIGURE 4: Resonance Raman spectra of different redox states of MauG. (A) Spectra of fully oxidized (a) and fully reduced (b) MauG. (B) Spectral changes occurring during reduction of MauG by incremental additions of sodium dithionite: fully oxidized MauG (a), partially reduced MauG (b and c), and fully reduced MauG (d). Protein concentrations were 0.25 mM.

that MauG has two heme centers with different structures. The set of marker bands at 1503 and 1588 cm^{-1} exhibits frequencies very similar to those of the ν_3 and ν_2 bands of *c*-type heme proteins with bis-histidine coordination (*12*−*16*) and strongly suggests that one heme center is a six-coordinate low-spin species with histidines as the proximal and distal axial ligands. The set of marker bands at 1478 and 1570 cm^{-1} is suggestive of a high-spin species. However, these bands are significantly lower in frequency than that of most high-spin *c*-type heme centers, which are normally five-coordinate (*17*). Since the ν_3 band from six-coordinate high-spin species normally appears at a lower frequency than that from a five-coordinate one (*18*, *19*), the ν_3 band at 1478 cm^{-1} may indicate that the high-spin heme is a six-coordinate species when oxidized.

When MauG is fully reduced by sodium dithionite, its RR spectrum (Figure 4A) shows a ν_4 band at 1359 cm^{-1} and two ν_3 bands at 1467 and 1492 cm^{-1}. The Raman band at 1492 cm^{-1} is coming from the reduced form of the low-spin heme center. The 1467 cm^{-1} band arises from the high-spin heme center; however, the frequency of this band now suggests a five-coordinate heme center (*17*). This result suggests that, upon reduction, the high-spin heme center in MauG undergoes a structural change that may involve displacement of a weak exogenous ligand such as water. Such a structural change will result in a vacant distal pocket for the high-spin heme in reduced MauG which may be important for substrate binding.

The results of the redox titration that was monitored by visible absorption spectroscopy (Figure 2) indicated that the two hemes of MauG were reduced to approximately the same extent during the reductive titration. This phenomenon was further investigated using another independent spectroscopic technique, RR spectroscopy, to monitor the reduction of MauG. RR spectroscopy may be performed in solution at ambient temperature so that the results can be directly compared and correlated with those of the redox titrations described above. It was not possible to directly monitor the potential and the RR spectrum simultaneously with our experimental setup. To address the question of whether the two hemes titrate individually and sequentially, or together, the overall redox state of MauG was referenced to the changes in the ν_4 band which shifts from 1374 cm^{-1} in oxidized MauG to 1359 cm^{-1} in fully reduced MauG. Figure 4B shows the RR spectral changes which occur during a reductive titration with sodium dithionite. When MauG is in intermediate stages of reduction, as judged by the shift and broadening in the ν_4 band, the ν_3 bands from both heme centers at 1478 and 1503 cm^{-1} shift to 1467 and 1492 cm^{-1}, respectively, at the same time during the reduction process. These data confirm that the two hemes of MauG are reduced in concert rather than sequentially during the reductive titration.

Spectrochemical Redox Titrations. The results described above indicate that the two hemes of MauG have distinct absorption and RR spectra but are reduced and oxidized together during the redox titrations. Intuitively, this suggests that the E_m values for the two hemes must be identical. To investigate this further, spectrochemical titrations of MauG were performed to precisely determine the E_m values associated with the different redox couples of MauG. Titrations were performed using FMN and safranin T as mediators (Figure 5). The fraction of reduced MauG was determined by the absorbance at either 550 or 406 nm.

Initial attempts to fit the data from spectrochemical titrations to the standard linear Nernst plot according to eq 3 consistently yielded plots which were slightly curved with slopes of approximately 90 mV (i.e., $n = 0.67$) (Figure 6).

$$E = E_m + (2.3RT/nF)\log([MauG_{ox}]/[MauG_{red}]) \quad (3)$$

This curvature, and a fitted *n* value much smaller than the known value of 1.0 for heme, suggested the possibility of negative cooperativity between the hemes. As such, the data were fit to eqs 1 and 2 which allow better visualization of the validity of alternative fits to a system with a single component or two distinct components. If the two hemes were equivalent and did not exhibit cooperativity, then the data would fit well to eq 1 and a fit to eq 2 would yield identical values for E_{m1} and E_{m2}. This was not the case. As indicated in Table 1, essentially identical results were obtained from analysis of the absorbance changes at either 550 or 406 nm, and in the presence or absence of safranin T in addition to FMN. This shows that the experimentally determined E_m values were not influenced by the redox dyes or interference in the analysis from spectral overlap. Data consistently yielded better fits to eq 2, which assumes an *n* value of 1.0 for each heme, with E_m values of -159 ± 10 and -244 ± 5 mV versus the NHE (Figure 7).

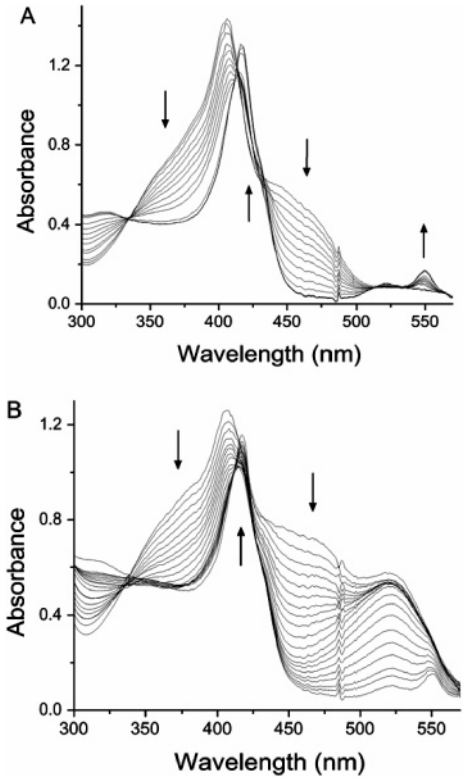

FIGURE 5: Spectrochemical titrations of MauG (5.0 μM) in the presence of FMN (40 μM) as a mediator (A) and in the presence of FMN (50 μM) and safranin T (16 μM) as mediators (B). The arrows indicate the direction of the spectral changes during the titration in the reductive direction.

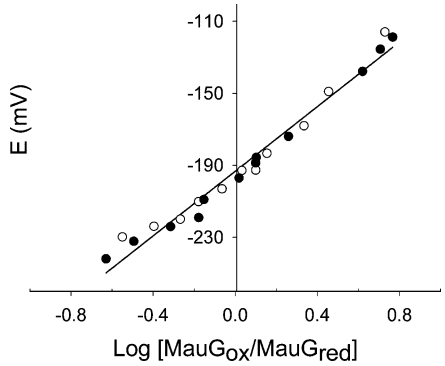

FIGURE 6: Nernst plot for the reductive titration of MauG in the presence of FMN as a mediator. Experimental points from the forward and reverse reductive (●) and oxidative (○) titrations are shown. Values of log[MauG$_{ox}$]/[MauG$_{red}$] were obtained from the absorbance changes at 550 nm. The straight line shows the fit of these data to eq 3 which yields a slope of 90 mV (n = 0.67) and an intercept of −193 mV.

Direct Electrochemistry of MauG. The redox properties of MauG were also analyzed by cyclic voltammetry at a SWNT-modified electrode (Figure 8A). The complexity of the system described in the spectrochemical studies is also evident in these data. The asymmetric cathodic (upper) peak is also suggestive of negative cooperativity. Computer simulations of the electrochemical data were performed to determine the basis for this asymmetry. The simulation which was most consistent with the experimental data describes a mechanism which occurs in three stages. The first step is an electrochemical process which involves the transfer of an electron to the protein at the electrode surface. This gives rise to a product which is converted into a second species which is itself electrochemically active within the potential window used in the experiment. A model consistent with this mechanism for MauG is shown in Figure 9. It should be noted that it was possible to obtain only qualitative support for this model using these data. A more quantitative simulation required knowledge of parameters which could not be determined such as the surface concentration of the electroactive proteins. Another problem is that theoretical models of electron transfer kinetics that have been established for planar electrodes are not necessarily applicable to the surface of the SWNT-modified electrode.

Table 1: E_m Values Obtained from Spectrochemical Titrations of MauG[a]

mediator	wavelength (nm)[b]	E_{m1} (mV)	E_{m2} (mV)
FMN	550	−240 ± 4	−159 ± 9
FMN	406	−247 ± 5	−159 ± 14
FMN and safranin T	406	−246 ± 5	−159 ± 4

[a] E_m values were obtained by fitting the experimental data from titrations shown in Figure 7 and similar experiments to eq 2. [b] The concentrations of the oxidized and reduced MauG were determined by comparison with the spectra of the completely oxidized and reduced forms of MauG at the indicated wavelength.

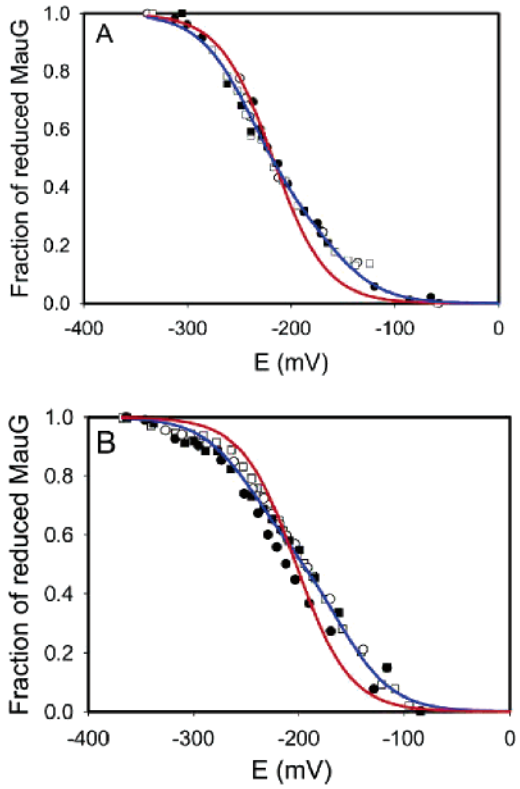

FIGURE 7: Determination of E_m values of MauG. In each experiment, the MauG sample was fully reduced by incremental addition of sodium dithionite (●), then fully oxidized by incremental addition of ferricyanide (○), then re-reduced by incremental addition of sodium dithionite (■), and then reoxidized by incremental addition of ferricyanide (□). The sets of data from each of these four reversible titrations are overlaid and were all included in the analysis. The fits of these data to eqs 1 (red line, one-component fit) and 2 (blue line, two-component fit) are shown. (A) This titration was performed in the presence of FMN as a mediator, and the fraction of MauG reduced was calculated from the spectral changes at 550 nm. (B) This titration was performed in the presence of FMN and safranin T as mediators, and the fraction of MauG reduced was calculated from the spectral changes at 406 nm.

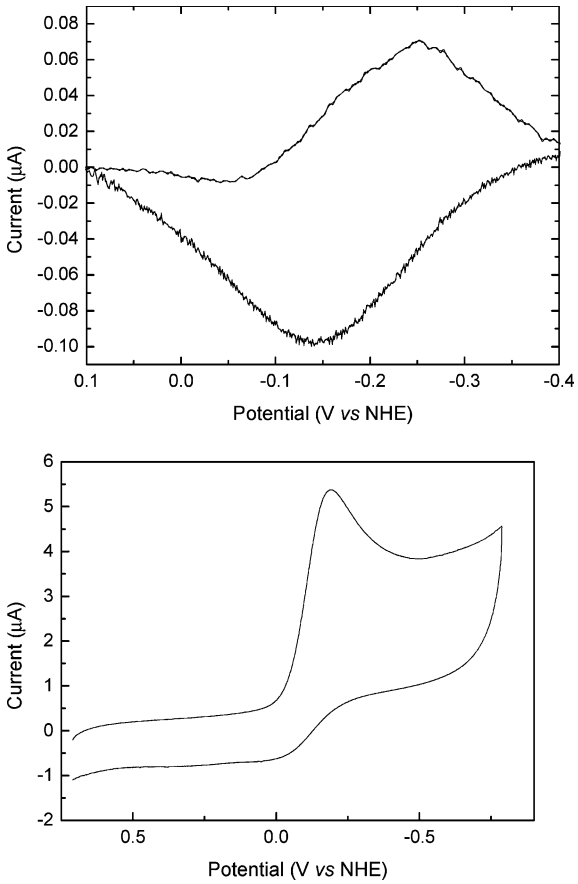

FIGURE 8: (A) CV of MauG on a SWCN modified electrode in pH 7.5 buffer under anaerobic conditions. (B) CV of MauG on a SWCN modified electrode in pH 7.5 buffer in the presence of oxygen.

Although it was not possible to distinguish the two individual E_m values by this technique, a single average E_m value of −198 mV versus the NHE could be determined anaerobically at pH 7.5. This correlates very closely with the results of the spectrochemical titrations as this value is approximately equal to the average of the two E_m values that were obtained in the spectrochemical study.

In the presence of oxygen, the CV of MauG (Figure 8B) shows a catalytic reduction peak of oxygen which is a characteristic of oxygen-binding heme proteins such as myoglobin and hemoglobin. This provides additional evidence of the oxygen binding property of MauG.

DISCUSSION

The data obtained during the spectrochemical titrations of MauG are clearly best fit to a two-component model with E_m values of −159 and −244 mV. If these E_m values described each of the two hemes of MauG in the absence of any cooperativity or interaction between hemes, then at the midpoint in the overall redox titration one heme should be predominantly reduced and the other predominantly oxidized. If the two hemes were reduced sequentially, then the difference spectra for the first and second halves of the titration should be identical only if the two hemes possess identical spectra. The high- and low-spin hemes of MauG have different spectral properties (Figures 2 and 4), yet the data for MauG do show that these two difference spectra are essentially identical. Thus, the two hemes of MauG with distinct spectra appear to be reduced simultaneously, despite the observation of two E_m values for the overall oxidation−reduction reaction of MauG. This means that it is inappropriate to assign each of the E_m values to one heme or the other. Instead, the E_m values should be viewed as describing the first and second one-electron reductions of an interacting diheme system.

A model that describes the redox behavior of MauG under anaerobic conditions is given in Figure 9. In this model, the intrinsic E_m value of each heme is very similar. The hemes are designated H1 and H2 since it is not possible to distinguish which serves as the point of entry of the electron into MauG. After the first electron reduces the first heme of MauG, that electron rapidly equilibrates between the two hemes. The E_m value associated with this first one-electron reduction of MauG is −159 mV. Once the first electron enters the system, this makes the further reduction of MauG more difficult, possibly due to electrostatic considerations. The E_m value associated with the second one-electron reduction is −244 mV. Thus, the two redox potentials do not describe redox properties of distinct hemes, but the first and second one-electron reductions of a diheme system with two hemes with similar intrinsic redox properties. Such behavior may be described as negative cooperativity.

The model in Figure 9 requires that the two hemes of MauG be well-coupled and suggests that they are positioned or oriented such that rapid electron transfer from one heme to the other may occur. This has mechanistic consequences. The mechanism by which MauG catalyzes the incorporation of oxygen into the biosynthetic precursor of TTQ has not yet been determined. A model for the activation of O_2 by MauG that is based on the proposed mechanism of cytochrome P450 enzymes and other heme-containing oxygenases (*20*) is shown in Figure 10. The high-spin and low-spin hemes are designated $Heme_H$ and $Heme_L$, respectively. The reduced high-spin heme binds dioxygen and transfers an electron to it, resulting in a covalent ferric−superoxide intermediate. This is followed by intra-heme electron transfer followed by delivery of the second electron to this intermediate to form a ferric−peroxide intermediate. In the presence of a substrate, it is possible that this intermediate is directly

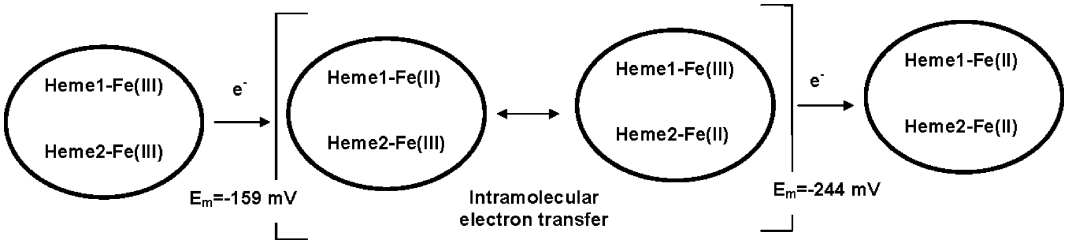

FIGURE 9: Model for cooperative redox behavior during the anaerobic reduction of MauG.

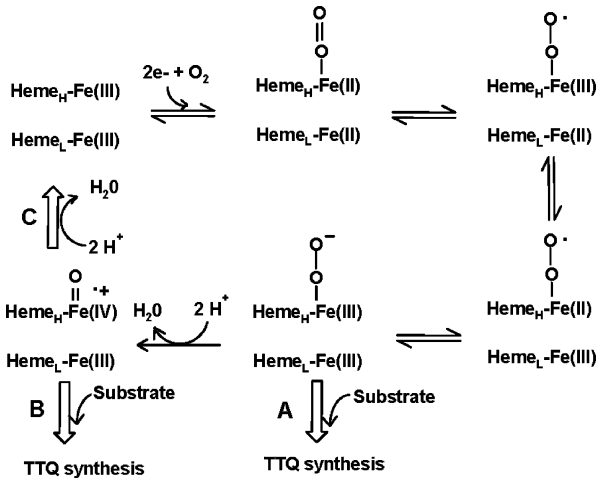

FIGURE 10: Possible reaction intermediates during the redox cycle of MauG in the presence of oxygen and substrate. Heme$_H$ and Heme$_L$ designate the high-spin and low-spin heme, respectively. A−C designate possible reactions involving intermediates which are described in the text.

involved in the oxygenation reaction required for TTQ biosynthesis (reaction A in Figure 10). Alternatively, this intermediate may convert to an oxo−ferryl intermediate which is used for the biosynthetic oxygenation reaction (reaction B in Figure 10). Thus, while oxygen is bound to the high-spin heme, the strong interaction with the low-spin heme allows the oxygen-binding heme to effectively function as a two-electron reductant. The ability to efficiently deliver the second electron to the ferric−superoxide intermediate may be important mechanistically for two reasons. It prevents dioxygen from being released after reversible binding, thus effectively enhancing the affinity of reduced MauG for O_2. It also prevents the accumulation of the potentially toxic superoxide intermediate which could potentially damage the host protein. In the absence of a substrate, fully oxidized MauG may be regenerated by reaction C in Figure 10. This accounts for the observation that reduced MauG is reoxidized by air (*1*).

In general, deviations from simple Nernstian behavior in a system with multiple redox centers may be due to either intrinsic differences in the E_m values of the redox centers or cooperative interactions between the redox centers. Evidence has been presented for cooperative interactions in some proteins which possess multiple *c*-type hemes. Examples include the diheme cytochrome c_4 (*21*) and the tetraheme cytochrome c_{554} from *Nitrosomonas europa* (*22*, *23*). In contrast to MauG, these multiheme *c*-type cytochromes function solely as electron transfer mediators. MauG exhibits some sequence similarity to diheme cytochrome *c* peroxidases (*1*). These proteins also possess both high- and low-spin *c*-type hemes (*24*, *25*). In contrast to those of MauG, the E_m values of these two hemes are not equivalent but are separated by several hundred millivolts. Thus, among the multi-*c*-type heme proteins which have been characterized thus far, MauG remains unique in that it seems to take advantage of redox cooperativity between two *c*-type hemes to allow for activation of O_2 by the high-spin heme. This description of MauG does bear a strong similarity to the redox cooperativity that has been described for cytochrome *c* oxidase. Cooperative interactions between cytochrome *a* and cytochrome a_3 of cytochrome *c* oxidase have long been thought to play an important role in the mechanism of that complex redox enzyme (*26*−*28*). In this case, rapid inter-heme electron transfer is important for the catalytic reduction of O_2 which occurs at the cytochrome a_3/Cu_B site. It has also been demonstrated that the relative timing of delivery of electrons and protons to this site of reaction is critical for achieving catalysis rather than suicide inactivation which likely results from damage from a reactive oxygen intermediate (*29*). Thus, the type of redox cooperativity described in this study may be of general importance to cofactor−cofactor interactions in enzymes which use a one-electron redox center to activate dioxygen.

The structure of MauG is not known, but it is known from the sequence that each heme possesses at least one His axial ligand. The sequence contains two CXXCH motifs which are diagnostic of a *c*-type heme with covalent attachment via the two Cys residues and with the His following the second Cys serving as an axial ligand. The RR spectrum and E_m value for the low-spin six-coordinate heme suggest that a second His serves as the second axial ligand. E_m values for most His−Met *c*-type hemes are greater than 200 mV, while those of His−His hemes are negative (*30*). The previously published EPR data for MauG (*1*) are also consistent with an imidazolate distal ligand. The E_m value for the high-spin five-coordinate heme is somewhat negative compared to those of other five-coordinate hemes with an axial His ligand which usually have positive E_m values (*30*). An exception is the five-coordinate heme of diheme cytochrome *c* peroxidase which exhibits an E_m of −260 mV (*24*). This suggests that in MauG the protein environment of the proximal His ligand of the high-spin heme, and possibly hydrogen bond interactions, are responsible for the relatively negative E_m value. Oxygen activation by heme proteins is typically catalyzed by cytochrome P450 enzymes. The heme cofactors of cytochrome P450 enzymes possess a single axial ligand that is provided by a Cys residue. In MauG, the only Cys residues that are present in the sequence are those in the CXXCH motifs which are predicted to be involved in the covalent thioether linkage between the protein and the heme. Thus, it is not possible for Cys to provide an axial ligand for either heme of MauG. The results of this study suggest that O_2 activation by MauG is catalyzed by a five-coordinate high-spin *c*-type heme, with a single His axial ligand, which interacts closely with a second *c*-type heme. This suggests an atypical mechanism for a heme-catalyzed oxygenation reaction. Efforts to obtain the structure of MauG are in progress, and additional studies are planned to further elucidate the physical properties and catalytic mechanism of MauG.

ACKNOWLEDGMENT

We thank Yu Tang for technical assistance and Jonathan Hosler for helpful discussion.

REFERENCES

1. Wang, Y., Graichen, M. E., Liu, A., Pearson, A. R., Wilmot, C. M., and Davidson, V. L. (2003) MauG, a novel diheme protein required for tryptophan tryptophylquinone biogenesis, *Biochemistry 42*, 7318−7325.
2. McIntire, W. S., Wemmer, D. E., Chistoserdov, A., and Lidstrom, M. E. (1991) A new cofactor in a prokaryotic enzyme: Tryptophan tryptophylquinone as the redox prosthetic group in methylamine dehydrogenase, *Science 252*, 817−824.

3. Davidson, V. L. (2001) Pyrroloquinoline quinone (PQQ) from methanol dehydrogenase and tryptophan tryptophylquinone (TTQ) from methylamine dehydrogenase, *Adv. Protein Chem. 58*, 95−140.
4. Pearson, A. R., de la Mora-Rey, T., Graichen, M. E., Wang, Y., Jones, L. H., Marimanikkupam, S., Aggar, S. A., Grimsrud, P. A., Davidson, V. L., and Wilmot, C. M. (2004) Further insights into quinone cofactor biogenesis: Probing the role of mauG in methylamine dehydrogenase TTQ formation, *Biochemistry 43*, 5494−5502.
5. Wang, Y., Li, X., Jones, L. H., Pearson, A. R., Wilmot, C. M., and Davidson, V. L. (2005) MauG-dependent in vitro biosynthesis of tryptophan tryptophylquinone in methylamine dehydrogenase, *J. Am. Chem. Soc. 127*, 8258−8259.
6. van der Palen, C. J., Reijnders, W. N., de Vries, S., Duine, J. A., and van Spanning, R. J. (1997) MauE and MauD proteins are essential in methylamine metabolism of *Paracoccus denitrificans*, *Antonie Van Leeuwenhoek 72*, 219−228.
7. van der Palen, C. J., Slotboom, D. J., Jongejan, L., Reijnders, W. N., Harms, N., Duine, J. A., and van Spanning, R. J. (1995) Mutational analysis of mau genes involved in methylamine metabolism in *Paracoccus denitrificans*, *Eur. J. Biochem. 230*, 860−871.
8. Husain, M., Davidson, V. L., and Smith, A. J. (1986) Properties of *Paracoccus denitrificans* amicyanin, *Biochemistry 25*, 2431−2436.
9. Cammack, R. (1995) in *Bioenergetics: A Practical Approach* (Brown, G. C., and Cooper, C. E., Eds.) pp 85−109, IRL Press, New York.
10. Liu, Z., Shen, Z., Zhu, T., Hou, S., Ying, L., Shi, Z., and Gu, Z. (2000) Organizing single-walled carbon nanotubes on gold using a wet chemical self-assembling technique, *Langmuir 16*, 3569−3573.
11. Feng, M., and Tachikawa, H. (2001) Raman spectroscopic and electrochemical characterization of myoglobin thin film: Implication of the role of histidine 64 for fast heterogeneous electron transfer, *J. Am. Chem. Soc. 123*, 3013−3020.
12. Chottard, G., Kazanskaya, I., and Bruschi, M. (2000) Resonance Raman study of multihemic *c*-type cytochromes from *Desulfuromonas acetoxidans*, *Eur. J. Biochem. 267*, 1050−1058.
13. Andersson, K. K., Babcock, G. T., and Hooper, A. B. (1984) Diheme cytochrome *c*-554 from *Nitrosomonas*. Soret resonance Raman indication of an unusual ferric 5-coordinate structure, *FEBS Lett. 170*, 331−334.
14. Oellerich, S., Wackerbarth, H., and Hildebrandt, P. (2002) Spectroscopic characterization of nonnative conformational states of cytochrome *c*, *J. Phys. Chem. B 106*, 6566−6580.
15. Eng, L. H., Schlegel, V., Wang, D., Neujahr, H., Stankovich, M. T., and Cotton, T. (1996) Resonance Raman scattering and surface enhanced resonance Raman scattering studies of oxidoreduction of cytochrome c_3, *Langmuir 12*, 3055−3059.
16. Verma, A. L., Kimura, K., Nakamura, A., Yagi, T., Inokuchi, H., and Kitagawa, T. (1988) Resonance Raman studies of hydrogenase catalyzed reduction of cytochrome c_3 by hydrogen. Evidence for heme heme interactions, *J. Am. Chem. Soc. 110*, 6617−6623.
17. Othman, S., Richaud, P., Vermeglio, A., and Desbois, A. (1996) Evidence for a proximal histidine interaction in the structure of cytochromes *c* in solution: A resonance Raman study, *Biochemistry 35*, 9224−9234.
18. Smulevich, G., Mauro, J. M., Fishel, L. A., English, A. M., Kraut, J., and Spiro, T. G. (1988) Heme pocket interactions in cytochrome *c* peroxidase studied by site-directed mutagenesis and resonance Raman spectroscopy, *Biochemistry 27*, 5477−5485.
19. Feng, M., Tachikawa, H., Wang, X., Pfister, T. D., Gengenbach, A. J., and Lu, Y. (2003) Resonance Raman spectroscopy of cytochrome *c* peroxidase variants that mimic manganese peroxidase, *J. Biol. Inorg. Chem. 8*, 699−706.
20. Sono, M., Roach, M. P., Coulter, E. D., and Dawson, J. H. (1996) Heme-containing oxygenases, *Chem. Rev. 96*, 28441−22887.
21. Leitch, F. A., Brown, K. R., and Pettigrew, G. W. (1985) Complexity in the redox titration of the dihaem cytochrome c_4, *Biochim. Biophys. Acta 808*, 213−218.
22. Arciero, D. M., Collins, M. J., Haladjian, J., Bianco, P., and Hooper, A. B. (1991) Resolution of the four hemes of cytochrome c_{554} from *Nitrosomonas europaea* by redox potentiometry and optical spectroscopy, *Biochemistry 30*, 11459−11465.
23. Upadhyay, A. K., Petasis, D. T., Arciero, D. M., Hooper, A. B., and Hendrich, M. P. (2003) Spectroscopic characterization and assignment of reduction potentials in the tetraheme cytochrome c_{554} from *Nitrosomonas europaea*, *J. Am. Chem. Soc. 125*, 1738−1747.
24. Arciero, D. M., and Hooper, A. B. (1994) A di-heme cytochrome *c* peroxidase from *Nitrosomonas europaea* catalytically active in both the oxidized and half-reduced states, *J. Biol. Chem. 269*, 11878−11886.
25. Gilmour, R., Goodhew, C. F., Pettigrew, G. W., Prazeres, S., Moura, I., and Moura, J. J. (1993) Spectroscopic characterization of cytochrome *c* peroxidase from *Paracoccus denitrificans*, *Biochem. J. 294*, 745−752.
26. Hendler, R. W., and Westerhoff, H. V. (1992) Redox interactions in cytochrome *c* oxidase: From the "neoclassical" toward "modern" models, *Biophys. J. 63*, 1586−1604.
27. Wikstrom, K. F., Harmon, H. J., Ingledew, W. J., and Chance, B. (1976) A re-evaluation of the spectral, potentiometric and energy-linked properties of cytochrome *c* oxidase in mitochondria, *FEBS Lett. 65*, 259−277.
28. Nicholls, P., and Petersen, L. C. (1974) Haem-haem interactions in cytochrome aa_3 during the anaerobic-aerobic transition, *Biochim. Biophys. Acta 357*, 462−467.
29. Mills, D. A., and Hosler, J. P. (2005) Slow proton transfer through the pathways for pumped protons in cytochrome *c* oxidase induces suicide inactivation of the enzyme, *Biochemistry 44*, 4656−4666.
30. Reedy, C. J., and Gibney, B. R. (2004) Heme protein assemblies, *Chem. Rev. 104*, 617−649.

BI052000N